

Distributed TES Model for Designing Low Noise Bolometers Approaching SAFARI Instrument Requirements

P. Khosropanah · R.A. Hijmering · M. Ridder · M.A. Lindeman · L. Gottardi · M. Bruijn · J. van der Kuur · P.A.J. de Korte · J.R. Gao · H. Hoervers

Received: 28 July 2011 / Accepted: 15 January 2012 / Published online: 27 January 2012
© The Author(s) 2012. This article is published with open access at Springerlink.com

Abstract Transition edge sensors (TES) are the chosen detector technology for the SAFARI imaging spectrometer on the SPICA telescope. The TES are required to have an NEP of $2\text{--}3 \times 10^{-19} \text{ W}/\sqrt{\text{Hz}}$ to take full advantage of the cooled mirror. SRON has developed TiAu TES bolometers for the short wavelength band (30–60 μm). The TES are on SiN membranes, in which long and narrow legs act as thermal links between the TES and the bath. We present a distributed model that accounts for the heat conductance and the heat capacity in the long legs that provides a guideline for designing low noise detectors. We report our latest results that include a measured dark NEP of $4.2 \times 10^{-19} \text{ W}/\sqrt{\text{Hz}}$ and a saturation power of about 10 fW.

Keywords Transition edge sensor · TES · Far infrared spectrometer · Submm spectrometer · SiN membrane · Cryogenic detectors · THz detectors

1 Introduction

SPICA [1] is a Japanese-led mission to fly a 3.25 m diameter IR telescope with a cryogenically cooled mirror ($\sim 5 \text{ K}$). Cooling the optics reduces the background radiation caused by the ambient temperature of the FIR space telescopes that limits the sensitivity. The loading is then dominated by astrophysical background sources. The SAFARI [2] instrument is an imaging Fourier Transform Spectrometer (FTS) on SPICA with three bands covering the wavelength ranges: 35–60 μm , 60–110 μm ,

P. Khosropanah (✉) · R.A. Hijmering · M. Ridder · M.A. Lindeman · L. Gottardi · M. Bruijn · J. van der Kuur · P.A.J. de Korte · J.R. Gao · H. Hoervers
SRON Netherlands Institute for Space Research, Sorbonnelaan 2, 3584 CA Utrecht, The Netherlands
e-mail: p.khosropanah@sron.nl

J.R. Gao
Kavli Institute of NanoScience, Delft University of Technology, Lorentzweg 1, 2628 CJ Delft, The Netherlands

and 110–210 μm . The background radiation in these bands is estimated by emission from the Zodiacal light at a level of 0.3–1 fW. [2] This gives a photon noise equivalent power (NEP) at the detectors of $\sim 2\text{--}3 \times 10^{-19} \text{ W}/\sqrt{\text{Hz}}$. Therefore, we require detectors with electrical NEPs at least lower than the photon noise limit, i.e. $\leq 3 \times 10^{-19} \text{ W}/\sqrt{\text{Hz}}$. This is about 2 orders of magnitude higher sensitivity than what is required for detectors on a ground based telescope and impose a great challenge on the detector technology.

Transition edge sensor (TES) is the chosen detector for the SAFARI instrument. In collaboration with several European institutes, SRON is developing low thermal conductance TES bolometers that are based on Ti/Au bilayer as the sensitive element on suspended silicon nitride (SiN) membranes. The measured dark NEPs in our original devices were typically a factor of 2–3 higher than what were expected from the measured thermal conductance [3]. Here we argue that part of the excess noise is due to the thermal fluctuation in the supporting legs and present a distributed leg model that provides a guideline for designing low noise devices. We then support the model by our latest measurement results.

2 Distributed Model

The simplest TES model consists of a heat capacity C_{TES} connected to the bath with a heat conductance G_{TES} . The electrical-thermal equations that follow from this model were introduced by M.A. Lindeman [4]. In the low- G devices as the legs are very long the mass and the heat capacity of the legs are considerable compared to that of the TES and the SiN island. The temperature along the legs also varies between the T_C and the T_{bath} . A way to model this would be to consider the legs as a series of bodies with certain heat capacities C 's at different temperature that are connected with series of G 's as shown in Fig. 1. The total heat conductance is then $G_{TES} = G/(n + 1)$. Similarly, the total heat capacity of the legs is $C_{LEG} = nC$, where n is the number the segments chosen for a SiN leg. A more comprehensive model would take into account the temperature dependence of C 's and G 's and assign different values to different bodies. Also we assume a linear temperature distribution between the bodies from T_C to T_{bath} , which further simplifies the model. Writing the small signal heat balance equations similar to the simple model leads us the following impedance matrix that can be used to calculate the noise, responsivity and the complex impedance of the TES.

In Fig. 1 R_L is the loading resistance and L is the inductance in the bias circuit. T_0 is the temperature of the device, R_0 is the resistance of the TES, I_0 is the dc current that runs through the device and P_0 is the corresponding dc power. α and β are defined as:

$$\alpha = \left. \frac{T_0}{R_0} \frac{\partial R}{\partial T} \right|_{I_0}, \quad \beta = \left. \frac{I_0}{R_0} \frac{\partial R}{\partial I} \right|_{T_0}.$$

The total noise current consists of the phonon noise I_{PH} , the Johnson noise I_{JO} and the noise from the loading resistor I_L .

$$I_{TOTAL}(\omega) = \sqrt{I_{PH}^2(\omega) + I_{JO}^2(\omega) + I_L^2(\omega)},$$

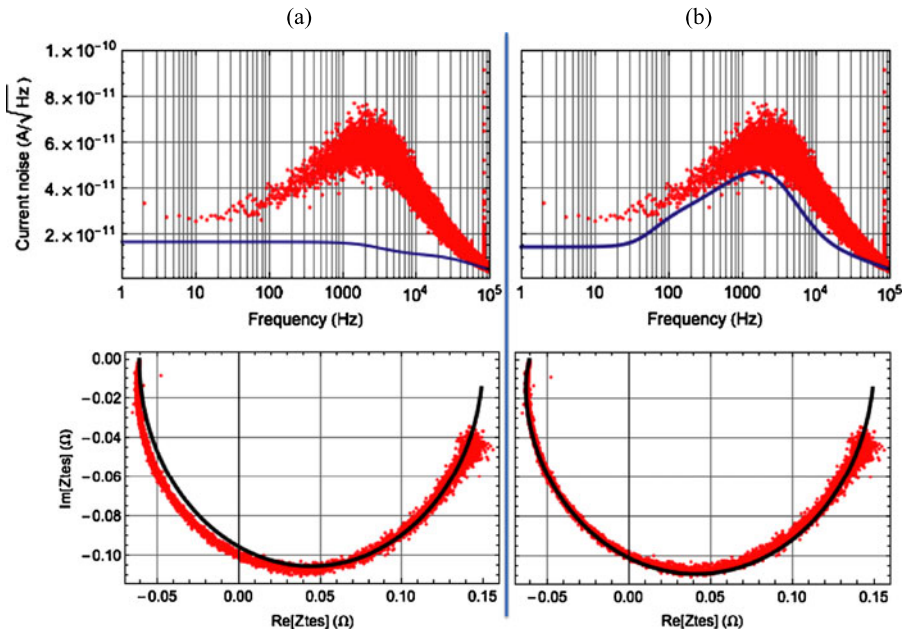


Fig. 2 (Color online) Measured (*red dots*) noise and complex impedance compared with calculated (*solid lines*) values using (a) simple TES model ($n = 0$) and (b) distributed leg model ($n = 10$). The bias point is at 30% of the normal state resistance

into 10 bodies and insert it between the TES and the bath. The number 10 is chosen as an example and by no means is an optimal. We ran the model for up to 10 bodies and see that the results converge slowly. Increasing the number of bodies further has to be investigated but we do not expect a drastic change in results and the conclusions certainly remain the same. As we see in Fig. 2 (a) and (b), the measured noise is about a factor of two higher than the calculated noise at low frequencies. Besides, there is a bump in the measured noise spectra that cannot be explained by the simple model and there is a clear difference between the measured and modeled impedance curves at low frequencies. Although the distributed leg model cannot explain all the excess noise, it does predict the shape of the noise spectra and is in better agreement with the measured impedance. Overall our modeling effort indicates that the major part of our excess noise is due to the thermal fluctuations in the long supporting legs.

3 Low Noise Design Guideline

The measured NEP of the TES in Fig. 2 is $2 \times 10^{-18} \text{ W}/\sqrt{\text{Hz}}$, which is about an order of magnitude higher than what is required for the SAFARI. In order to reduce the NEP we need to lower the G_{TES} . Assuming that G_{TES} scales with the leg geometry this can be realized by combination of increasing the length, decreasing the width and reducing the membrane thickness.

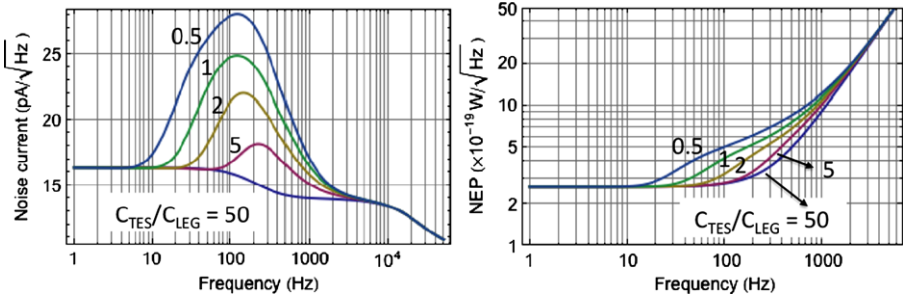


Fig. 3 (Color online) Calculated noise and NEP using the distributed model ($n = 10$) for different heat capacity in the legs. In all cases the heat capacity of TES (C_{TES}) is 5 fJ/K and total heat conductance is 0.3 pW/K. The bias point is at 30% of the normal state resistance

Table 1 Parameters of the devices

Parameter	TES #1	TES #2
Leg length [μm]	1310	400
Leg width [μm]	6.5	1
Mem. thick. [μm]	1	0.5
TES size [μm^2]	110×110	50×50
Mem. size [μm^2]	140×140	160×160
T_C [mK]	75	78
R_N [m Ω]	212	103
Sat. power [fW]	9	10
G [pW/K]	0.38	0.33
NEP [$\text{W}/\sqrt{\text{Hz}}$]	6.5×10^{-19}	4.2×10^{-19}

In principle we can achieve a certain G_{TES} using different leg geometries and the distributed leg model enables us to calculate the noise for different designs. Figure 3 shows the calculated noise current spectra and the corresponding NEP for TES with the same G_{TES} but different leg mass. A T_C of 100 mK is used, which gives an NEP of about $3 \times 10^{-19} \text{ W}/\sqrt{\text{Hz}}$. Here the C_{TES} is set to 5 fJ/K but the total heat capacity of the legs (C_{LEG}) varies between 0.5 to 50 times smaller than C_{TES} .

It is clear that the lighter the legs, the lower the excess noise bump. The lower the total G_{TES} , the slower the device and therefore the noise roll-off frequency is lower. In case of very low- G devices with heavy legs, the low frequency tail of the noise bump can be stretched well below 10 Hz, where it merges with $1/f$ noise. As a result the measured dark NEP would be larger. To confirm this hypothesis we compare two devices one with heavy legs (TES #1) and the other one with light legs (TES #2). Table 1 summarized some of the important parameters of these two devices. As we see in Table 1, the T_C , saturation power and the G of these two are very similar but note that the legs of the TES #1 are about 42 times heavier than TES #2 (shown in Fig. 4). Although the membranes and the TES sizes are not the same, we believe that the main difference between the two devices is the mass of the legs. Figure 5 shows the noise current spectra at different bias points.

Fig. 4 (Color online) TES #2 fabricated on $0.5\ \mu\text{m}$ thick $160 \times 160\ \mu\text{m}^2$ SiN island supported by $1\ \mu\text{m}$ wide and $400\ \mu\text{m}$ long SiN legs

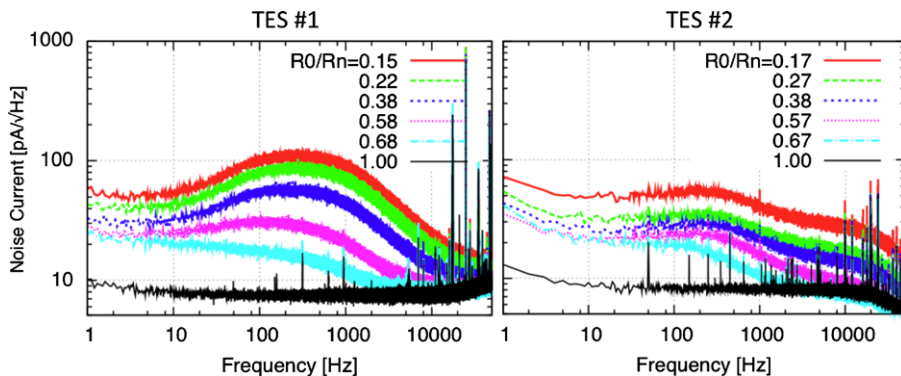
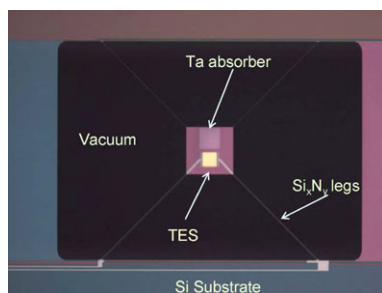


Fig. 5 (Color online) Noise current spectra of devices with heavy legs (TES #1) and light legs (TES #2). TES #1 has 42 times heavier legs than the TES #2

It is evident that the excess noise bumps seen in TES #1 are substantially smaller in TES #2 as expected from the model. We measured lower dark NEP of $4.2 \times 10^{-19}\ \text{W}/\sqrt{\text{Hz}}$ for the latter. The conclusion is that in order to achieve low NEP it is essential to fabricate low- G TES devices with as light as possible supporting legs. This means that they should be made as narrow as possible on as thin as possible membrane and only as long as necessary.

Acknowledgements The authors thank all the collaborators within ESA-TRP program for fruitful discussions, specially P. Mauskopf, D. Morozov from Cardiff University, S. Withington, D. Goldie, D. Glowacka, A. Velichko from University of Cambridge, A. Murphy, N. Trappe, C. O’Sullivan from National University of Ireland in Maynooth, D. Griffin from Rutherford Appleton Laboratory, B. Leone, P. Verhoeve and K. Isaak from ESA.

Open Access This article is distributed under the terms of the Creative Commons Attribution License which permits any use, distribution, and reproduction in any medium, provided the original author(s) and the source are credited.

References

1. H. Kaneda, T. Nakagawa, T. Onaka, T. Matsumoto, H. Murakami, K. Enya, H. Kataya, H. Matsuhara, Y.Y. Yui, in *Proc. SPIE Optical, Infrared, and Millimeter Space Telescopes*, vol. 5487 (2004), p. 991

2. B. Swinyard, in *Proc. SPIE Space Telescopes and Instrumentation I: Optical, Infrared, and Millimeter*, vol. 6265 (2006), p. 62650L
3. P. Khosropanah, B.P.F. Dirks, M. Parra-Borderías, M. Ridder, R. Hijmering, J. van der Kuur, L. Gottardi, M. Bruijn, M. Popescu, J.R. Gao, H. Hoevers, *IEEE Trans. Appl. Supercond.* **21**(3), 236 (2011)
4. M.A. Lindeman, S. Bandler, R.P. Brekosky, J.A. Chervenak, E. Figueroa-Feliciano, F.M. Finkbeiner, M.J. Li, C.A. Kilbourne, *Rev. Sci. Instrum.* **75**, 1283 (2004)
5. K.D. Irwin, G.C. Hilton, in *Cryogenic Particle Detection*. Topics in Applied Physics, vol. 99 (2005), p. 92
6. M.A. Lindeman, Ph.D. thesis (2000). Available online at: http://www.osti.gov/energycitations/product.biblio.jsp?osti_id=15009469